POLITECNICO
MILANO 1863

SCUOLA DI INGEGNERIA INDUSTRIALE
E DELL'INFORMAZIONE

Executive Summary of the Thesis

Generalised Conjugate Gradient for the minimisation of energy functionals in deformed nuclei

Laurea Magistrale in Nuclear Engineering - Ingegneria Nucleare

Author: Alessandro Sala

Advisor: Prof. Matteo Passoni

Co-advisor: Prof. Gianluca Colò

Academic year: 2024-2025

1. Introduction

The theoretical study of atomic nuclei provides a bridge between nuclear physics and nuclear engineering. Starting from a framework consistent with quantum mechanics, the strong interaction, and its underlying symmetries, modern nuclear theory aims to construct models characterised by a limited number of free parameters and capable of predicting both nuclear structure and reactions, across a wide range of systems. While experimental data have long provided invaluable insight into nuclear properties and processes, only a coherent theoretical description allows for systematic extrapolations towards regions of the nuclear chart or physical conditions that remain beyond current experimental reach, thus playing an essential role in applications relevant to nuclear engineering.

In particular, nuclear fission, despite its massive importance in nuclear engineering, remains only partially understood from a microscopic standpoint. Current models that use empirical approaches successfully reproduce global quantities like fission barrier heights, fragment mass distributions, and average neutron multiplicities for well studied nuclei. However, these models may rely on a huge number of parameters, which limit their predictive power when extrapolated to systems which are less investigated experimentally. A fully microscopic understanding of the collective dynamics leading from the compound nucleus to scission, the treatment of quantum many-body correlations, and the description of fragment excitation and emission remain among the major open challenges, particularly relevant for the simulation of next-generation reactors, which require the accurate description of nuclei and fuel materials – far less explored than those employed in traditional thermal systems – to be correctly predicted.

1.1. Microscopic description of nuclei

In this regard, the approach to the microscopic description of nuclei, is the one of the many-body theory, which starting from the interacting nucleons, aims at building a complete description of the nucleus. The use of phenomenological potentials based on the Woods-Saxon one is still relevant, thanks to its computational feasibility and its capability to include shell effects in a simple manner, but it cannot account for many-body effects. At the moment, there are two competing frameworks that try to tackle the microscopic description of nuclei, (a) the *ab-*

initio approach, where the interaction is in principle exact, derived from controlled approximations of quantum chromodynamics; and (b) the use of effective interactions and nuclear Density Functional Theory.

Ab-initio methods Ab-initio methods, while technically speaking more rigorous, are still limited as of now, since they can only account for light nuclei or medium-heavy nuclei that can be considered as spherical. Energy density functionals and effective interactions, such as the Skyrme force, on the other hand are more flexible and less computationally expensive, enabling a much wider representation of nuclei across the whole chart, including heavy nuclei and processes such as fission, fusion, reactions and decays, which are of crucial importance in nuclear engineering.

Density Functional Theory D Vautherin and D M Brink laid the foundations of the nuclear Hartree–Fock theory using the Skyrme interaction in 1972 [5], through spherically symmetric calculations, which are unable to account for nuclear deformations, essential for nuclei far from magic numbers. Over the years, thanks to the increase in computational performance of modern hardware, codes that are able to represent more coordinates have been written, mainly using basis expansions on the harmonic oscillator, which have the downside of not being able to account for near drip line nuclei, due to the diffent asymptotic behaviour of the Gaussian basis in the harmonic oscillator and quasi-resonant states [2]. Thanks to the flexibility offered by nuclear DFT, it has been chosen in the present work as the framerowk of choice. In particular, using an Energy Density Functional (EDF) derived inspired by the Hartree–Fock expectation value of the Skyrme interaction.

2. Objective and methods

The aim of this work is to develop a new implementation of the Hartree–Fock method on an unconstrained 3D mesh, by the use of the Generalised Conjugate Gradient (GCG) method [3].

2.1. Objectives

The goals addressed by this work are the following:

- demonstrate the feasibility of the Generalised Conjugate Gradient for the solution of large-scale eigenvalue problems;
- solve the self-consistent Hartree–Fock equations on an unconstrained 3D mesh;
- verify the numerical accuracy of the new implementation, first against existing spherical codes;
- second against well established deformed codes; and
- attempt to produce novel results that specifically require an unconstrained implementation of this kind, and establish the advance brought to the field by this work.

2.2. Methods

Skyrme Energy Functional The many-body nuclear problem is approached within the Hartree–Fock framework, described in section **??**. As discussed in chapter **??**, a pure HF treatment is not sufficient for a quantitative description of nuclear structure, and a more general energy density functional (EDF) formulation must be adopted. In this work, we employ the Skyrme EDF, whose construction and resulting mean-field equations are developed in section **??**. This provides the self-consistent single-particle Hamiltonian that forms the basis for the numerical treatment.

Finite Differences and Generalised Conjugate Gradient Once the equations to be solved have been derived, their numerical solution requires both a spatial discretization scheme and an efficient solver for the large-scale eigenvalue problem that arises at each iteration of the self-consistent procedure.

3. Theoretical framework

The energy functional to be minimised is of the form [1]

$$E_{\mathrm{HF}} = \int (\mathcal{E}_{\mathrm{Kin}} + \mathcal{E}_{\mathrm{Skyrme}} + \mathcal{E}_{\mathrm{Coul}}) d\boldsymbol{r}.$$

3.1. Skyrme Functional

The Skyrme functional formulation used is the following [4]:

$$\mathcal{E}_{\text{Skyrme}} = \sum_{t=0,1} \Big\{ C_t^{\rho}[\rho_0]\rho_t^2 + C_t^{\Delta\rho}\rho_t\nabla^2\rho_t + \\ + C_t^{\nabla\cdot J}\rho_t\nabla\cdot\mathbf{J}_t + C_t^{\tau}\rho_t\tau_t \Big\}$$

3.2. Coulomb treatment

Unlike the Skyrme interaction, the Coulomb force is finite-range, giving rise to an unwanted integral operator in the single-particle Hamiltonian. A well known and widely used device is the Slater approximation [**?**], which gives a local exchange interaction. In this approximation, the Coulomb energy reads

$$E_{\text{Coul}} = \int \mathcal{E}_{\text{Coul}}(\mathbf{r})d\boldsymbol{r}$$

where the energy density is given by

$$\mathcal{E}_{\text{Coul}}(\boldsymbol{r}) = \frac{e^2}{2}\left[\int \frac{\rho_p\rho_p'}{|\mathbf{r}-\mathbf{r}'|}d\mathbf{r}' - \frac{3}{2}\left(\frac{3}{\pi}\right)^{\frac{1}{3}}\rho_p^{4/3}\right]. \tag{1}$$

which results in the Coulomb potential field

$$U_C(\mathbf{r}) = \frac{e^2}{2}\left[\int \frac{\rho_p(\mathbf{r}')}{|\mathbf{r}-\mathbf{r}'|}d^3\mathbf{r}' - 2\left(\frac{3}{\pi}\right)^{\frac{1}{3}}\rho_p^{1/3}(\mathbf{r})\right] \tag{2}$$

Given the proton density, we can impose Dirichlet boundary conditions, which can be extracted from a quadrupole expansion of the charge density [**?**]

$$V_c(\mathbf{r}) = 4\pi e^2\sum_{\lambda=0}^{2}\sum_{\mu=-\lambda}^{\lambda}\frac{\langle Q_{\lambda\mu}\rangle Y_{\lambda\mu}}{r^{1+\lambda}} \text{ on } \partial\Omega \tag{3}$$

4. Numerical Implementation

4.1. Finite Differences

Given that the whole equation is linear in φ, we can evaluate it on the chosen mesh, using finite differences to approximate the differential operators, yielding a linear eigenvalue problem of the form

$$\sum_{\alpha=1}^{N} A_{\alpha\beta}\varphi_\beta = E\varphi_\alpha \tag{4}$$

where the shorthand notation $N = 2\cdot N_x\cdot N_y\cdot N_z$ is used to denote the size of the matrix A, which is $N \times N$.

4.2. Generalised Conjugate Gradient

The novel Generalised Conjugate Gradient is implemented [3].

5. Benchmarks

5.1. Spherical nuclei

Physical quantities

		GCG	hfbcs_qrpa
E_{TOT}	[MeV]	-128.402	-128.400
$\langle r_n^2\rangle^{1/2}$	[fm]	2.6584	2.6585
$\langle r_p^2\rangle^{1/2}$	[fm]	2.6835	2.6836
$\langle r_{ch}^2\rangle^{1/2}$	[fm]	2.7805	2.7803

Neutron energy levels

		GCG	hfbcs_qrpa
$1s_{1/2}$	[MeV]	-36.140	-36.137
$1p_{3/2}$	[MeV]	-20.611	-20.611
$1p_{1/2}$	[MeV]	-14.427	-14.428

Proton energy levels

		GCG	hfbcs_qrpa
$1s_{1/2}$	[MeV]	-32.349	-32.345
$1p_{3/2}$	[MeV]	-17.137	-17.137
$1p_{1/2}$	[MeV]	-11.081	-11.082

Table 1: ^{16}O complete of the Skyrme functional and Coulomb interaction.

Physical quantities

		GCG	hfbcs_qrpa
E_{TOT}	[MeV]	-783.587	-783.325
$\langle r_n^2\rangle^{1/2}$	[fm]	4.2854	4.2872
$\langle r_p^2\rangle^{1/2}$	[fm]	4.2196	4.2212
$\langle r_{ch}^2\rangle^{1/2}$	[fm]	4.2767	4.2704

Table 2: ^{90}Zr, box size [-15, 15] fm, step size 0.43 fm.

5.2. Deformed nuclei

Having established that the code works as expected for spherical nuclei, we can extend the calculations to deformed systems. In this chapter, the GCG implementation is validated against well-established deformed codes.

5.3. Basis code and ground state

		GCG no J^2	HFBTHO
E_{TOT}	[MeV]	-197.219	-197.030
$\langle r_n^2 \rangle^{1/2}$	[fm]	2.9998	2.9996
$\langle r_p^2 \rangle^{1/2}$	[fm]	3.0346	3.0326
$\langle r_{ch}^2 \rangle^{1/2}$	[fm]	3.1240	3.4614
$\langle \mathcal{Q}_{20} \rangle$	[-]	33.905	33.881

Table 3: Results for ^{24}Mg ground state, no pairing interaction, box $[-10, 10]$ fm, step size 0.33 fm, SkM* parametrisation.

Shell	$\lvert m_j \rvert$	E [MeV]
$1s_{1/2}$	1/2	-39.281
$1p_{3/2}$	1/2	-28.381
$1p_{3/2}$	3/2	-24.224
$1p_{1/2}$	1/2	-18.680
$1d_{5/2}$	1/2	-16.743
$1d_{5/2}$	3/2	-14.130

Table 4: Single-particle energy levels in the ground state of ^{24}Mg. As predicted by the Nilsson model, levels with a lower $|m_j|$ projection are lowered in energy, while those with a higher projection are raised, with respect to the spherical (degenerate) case.

5.4. Cartesian benchmark and deformation curve

$$\beta_2 = \frac{4\pi \langle \mathcal{Q}_{20} \rangle}{3AR^2} \tag{5}$$

Deformation curve, Constraints explaination

6. Original results

6.1. ^{20}Ne clustering

The formation of clusters in light nuclei has been a research focus object in recent years. The interest stems from different reasons. The formation of clusters at low density is a strong

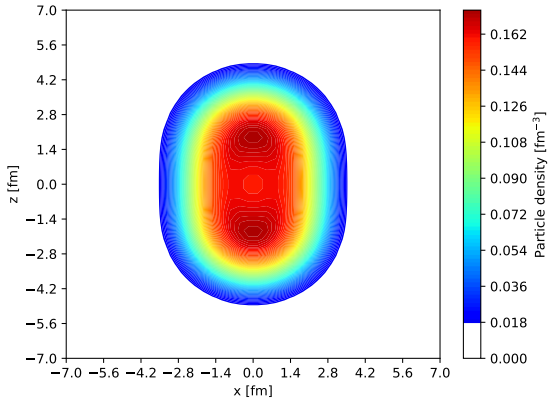

Figure 1: ^{24}Mg ground state density $\rho(x, 0, z)$, calculation done on a box $[-10, 10]$ fm, step size 0.33 fm, SkM* parametrisation.

indicator of specific correlations (n-p correlations or alpha-particle, ie 'quartetting' correlations) and a strong test for theory. At the same time, clustering may have impact on reactions and astrophysical processes [**?**]. It has to be noted that cluster formation during fission has been highlighted [**?**]. One of the hypothesis is that some light nuclei tend to form clusters of lighter particles, mainly α-particles, as to minimise their energy, by displaying 'molecular-like' bonds and resonances among the clusters. The phenomenon is not yet understood, with the following results we show that in the framework presented in this work, the formation of clusters is present in ^{20}Ne.

$$\tau_q^{\mathrm{TF}} = \frac{3}{5}(6\pi^2)^{2/3}\rho_q^{5/3}. \tag{6}$$

6.2. Near-drip line nuclei

The need of a mesh representation to account for weakly bound systems has been largely emphasised in previous chapters (see **??**, **??**). In this section, results regarding the two nuclei near drip line ^{42}Si and ^{28}S are presented, the former being a neutron-rich nucleus, the latter being a proton-rich nucleus. Being weakly bound systems, taking direct measurements of quantities like radii, deformations through spectroscopy etc, is not yet possible.

We shall compare the experimental neutron S_n or proton S_p separation energy with the theoretical value calculated using Koopmans' theorem [**?**]. The theorem states that in a frozen orbitals

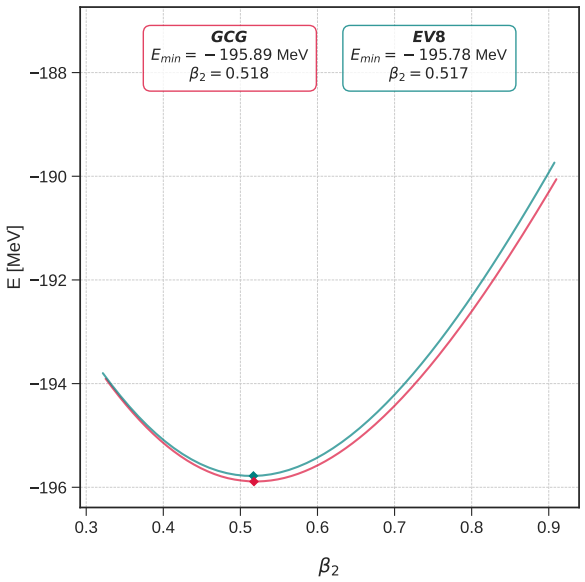

Figure 2: Comparison with the `EV8` code for ^{24}Mg, no pairing interaction, box $[-10, 10]$ fm, step size 0.6 fm, SLy4 parametrisation.

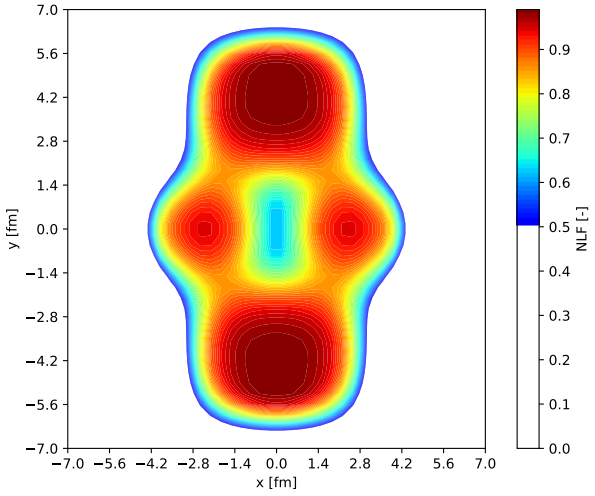

Figure 3: NLF, KDE33 functional.

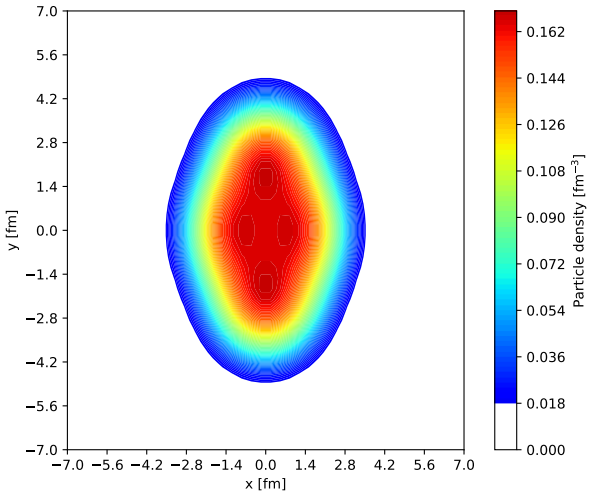

Figure 4: NLF, KDE33 functional.

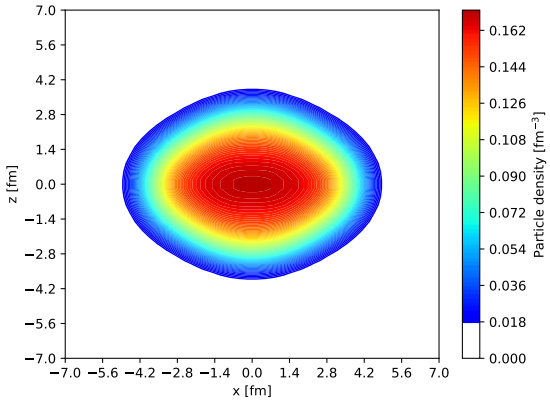

Figure 5: ^{42}Si density $\rho(x, 0, z)$, calculation done on a box $[-11, 11]$ fm, step size 0.37 fm, experimental data taken from [**?**].

approximation, where the mean-field is assumed to remain constant after the removal of a particle, the energy required to remove that particle is equal to the eigenvalue of the last occupied single-particle orbital with an opposite sign.

7. Conclusions

References

[1] M. Bender, P.-H. Heenen, and P.-G. Reinhard. Self-consistent mean-field models for nuclear structure. *Reviews of Modern Physics*, 75(1):121–180, 2003.

[2] G. Colò. Nuclear density functional theory. *Advances in Physics: X*, 5(1):1740061, 2020.

[3] Yu Li, Hehu Xie, Ran Xu, Chun'guang You,

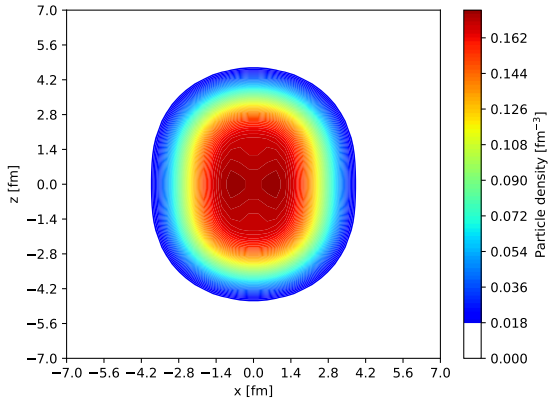

Figure 6: ^{28}S density $\rho(x, 0, z)$, calculation done on a box $[-10, 10]$ fm, step size 0.34 fm, experimental data taken from [**?**].

and Ning Zhang. A parallel generalised conjugate gradient method for large scale eigenvalue problems. *CCF Transactions on High Performance Computing*, 2(2):111–122, jun 2020. The corresponding computing package can be downloaded from the web site: `https://github.com/pase2017/GCGE-1.0`.

[4] P.D. Stevenson and M.C. Barton. Low-energy heavy-ion reactions and the skyrme effective interaction. *Progress in Particle and Nuclear Physics*, 104:142–164, 2019.

[5] D. Vautherin and D. M. Brink. Hartree–fock calculations with skyrme's interaction. i. spherical nuclei. *Phys. Rev. C*, 5:626–647, Mar 1972.